PROCEEDINGS OF SCIENCE

A statistical study of SDSS radio-emitters

Mariangela Vitale[*†a] **Jens Zuther,**[a] **Macarena García-Marín,**[a] **Andreas Eckart,**[ab] **Marcus Bremer,**[a] **Mónica Valencia-S**[a] **and Anton Zensus**[b]

[a] *I. Physikalisches Institut, Universität zu Köln, Zülpicher Strasse 77, 50937 Köln, Germany*
[b] *Max-Planck Instutut für Radioastronomie, Auf dem Hügel 69, 53121 Bonn, Germany*
E-mail: vitale@ph1.uni-koeln.de, zuther@ph1.uni-koeln.de, maca@ph1.uni-koeln.de, eckart@ph1.uni-koeln.de, mbremer@ph1.uni-koeln.de, mvalencias@ph1.uni-koeln.de, azensus@mpifr-bonn.mpg.de

The cross-correlation of the Sloan Digital Sky Survey Data Release 7 with the Faint Images of the Radio Sky at Twenty-Centimeters survey allows for a multiwavelength statistical study of radio-optical galaxy properties on a very large number of sources. The correlation we find between $L_{20\,\mathrm{cm}}/L_{\mathrm{H}\alpha}$ and optical emission line ratios suggests that the origin of the emission in powerful radio-galaxies is of nuclear rather than of stellar origin. In particular, the spectroscopic classification in Seyferts, Low Ionization Narrow Emission Regions (LINERs) and star-forming galaxies provided by emission-line diagnostic diagrams peaks on the AGN region for higher $L_{20\,\mathrm{cm}}/L_{\mathrm{H}\alpha}$ values. The trend differs from Seyferts to LINERs. The [NII]/Hα vs. equivalent width of the Hα line diagram confirms the LINER classification for most of those that have been identified with the traditional diagnostic diagrams. A small fraction of sources seem to be powered by post-AGB stars instead.

Nuclei of Seyfert galaxies and QSOs - Central engine & conditions of star formation
November 6-8, 2012
Max-Planck-Insitut für Radioastronomie (MPIfR), Bonn, Germany

[*] Speaker.
[†] International Max Planck Research School for Astronomy and Astrophysics at the Univerities of Bonn and Cologne, Auf dem Hügel 69, 53121 Bonn, Germany

PoS(Seyfert 2012)002

1. Introduction

Our knowledge of global galaxy properties has been recently improved thanks to large-area surveys such as the Sloan Digital Sky Survey (SDSS) [1]. The cross-correlation of the SDSS Data Release 7 (DR7) with the Faint Images of the Radio Sky at Twenty-Centimeters (FIRST) [2] survey offers the chance to study the optical properties of a large sample of radio emitters.
The intensity of optical emission lines in radio AGNs has been already investigated in the past [3 – 6]. The correlation between line strength and radio power suggests that optical and radio emission originate in the same physical process. However, the most powerful radio galaxies are generally detected at higher redshifts than the less powerful radio galaxies. This makes it difficult to establish whether there is a link between emission-line and radio luminosity, or between emission-line luminosity and redshift [7]. The finding of a high number of detected AGNs with increasing redshift is also supported by the downsizing scenario of galaxy evolution [8 – 10]. According to this scenario, galaxies placed at higher redshift are more massive and host black holes that accrete producing powerful jets.
AGNs can be selected from spectroscopic surveys using some optical emission line ratios. Low-ionization emission-line diagnostic diagrams [11] are used to point out the connection between the galaxy nuclear activity, its morphological type [12], and its evolutionary stage [13]. We make use of optical and radio data to conduct a statistical study on the prospects of identifying radio galaxies in some well-defined regions of the diagnostic diagrams.

2. Galaxy sample

The Sloan Digital Sky Survey (SDSS) is a photometric and spectroscopic survey that covers one-quarter of the celestial sphere in the north Galactic cap [1]. The spectra have an instrumental velocity resolution of $\sigma \sim 65$ km/s in the wavelength range $3800 - 9200$ Å. The identified galaxies have a median redshift of $z \sim 0.1$. Spectra are taken with $3''$ diameter fibers (5.7 kpc at $z \sim 0.1$). We make use of the Max-Planck-Institute for Astrophysics (MPA)-Johns Hopkins University (JHU) DR7 of spectrum measurements (http://www.mpa-garching.mpg.de/SDSS/DR7/). The catalog contains the derived galaxy properties of the $\sim 10^6$ sources from the SDSS DR7 [14].
The Faint Images of the Radio Sky at Twenty-Centimeters (FIRST) Survey [2] makes use of the Very Large Array (VLA) in the B-array configuration to produce a map of the 20 cm (1.4 GHz) sky emission with a beam size of $5''.4$ and an rms sensitivity of about 0.15 mJy/beam. The survey covers an area which corresponds to the sky regions investigated by SDSS, and includes $\sim 10^5$ sources.
The crosscorrelation of SDSS with the FIRST survey provides a large optical-radio sample of galaxies. For generating the cross-matched FIRST/SDSS sample, we used the matching results provided by the SDSS DR7 via Casjobs [15], based on a matching radius of $1''$. We apply the following conditions to our final sample: 1) $z > 0.04$ to avoid aperture effect [16] and 2) relative error on the EW measurements of lines involved in the diagnostic diagrams $< 30\%$. Our final cross-matched sample consists of 9 594 objects, which correspond to 25.6% of the full cross-matched optical-radio sample, 9.6% of the original radio sample (FIRST) and $\sim 1\%$ of all the galaxies in the MPA-JHU data release.

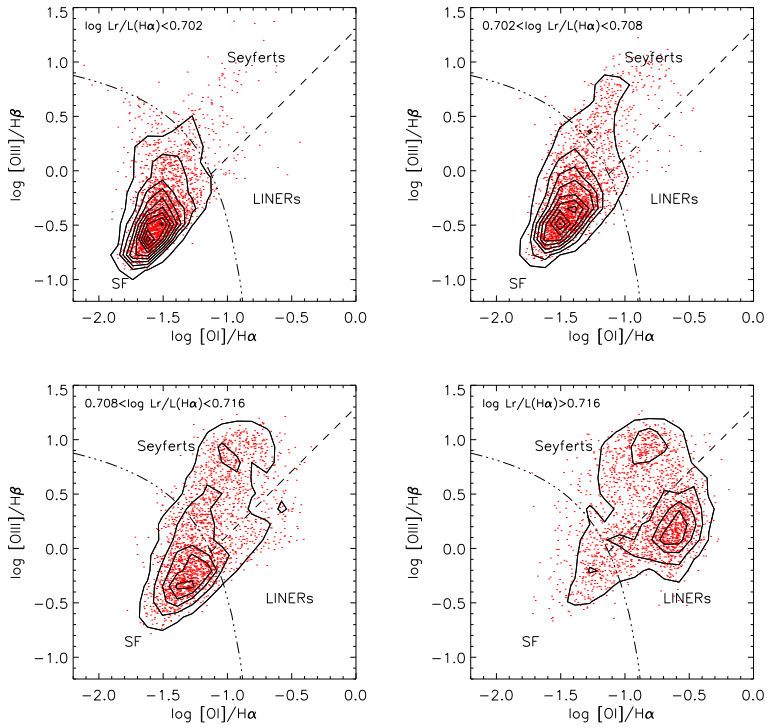

Figure 1: [OI]-based diagnostic diagrams. From top to bottom and from left to right, $\log(L_{20\ cm}/L_{H\alpha})$ increases. The number of radio emitters per bin is $2\,350 \pm 25$. The contours represent the number density of the radio emitters (20 galaxies per density contour).

3. Optical emission-line diagnostic diagrams

The Baldwin-Phillips-Terlevich (BPT) low-ionization diagnostic diagram [11] and its subsequent versions [17, 16, 18] make use of emission line ratios. The strength of a line ratio is considered to be either a function of the hardness of the ionizing field of the galaxy and the metallicity [19]. Higher ratios are assumed to mostly be the product of ionization that arises due to accretion around the black hole, rather than photoionization by hot massive OB stars. This diagnostic technique, largely used in the optical wavelength regime, allows differentiation of galaxies that show activity in their nuclei and starbursts. In particular, narrow-line AGN can be identified by the ratio of some distinctive emission-lines, such as [OI] λ6300 Å over H$\alpha\lambda$6563 Å and [OIII] λ5007 Å over H$\beta\lambda$4861 Å.

Transitions requiring relatively high ionization potential are found to happen in powerful radio emitters [20, 21, 4, 22, 23], pointing to a possible correlation between AGN-detection rate and radio luminosity of the host galaxies. Some of the AGN and composite galaxies with widely spread distributions of metallicity and ionization parameters are degenerate with star-forming galaxies. This is especially the case of the [OI]/Hα versus [OIII]/Hβ diagram, which is particularly sensitive to shock excitation coming from either AGN or stars.

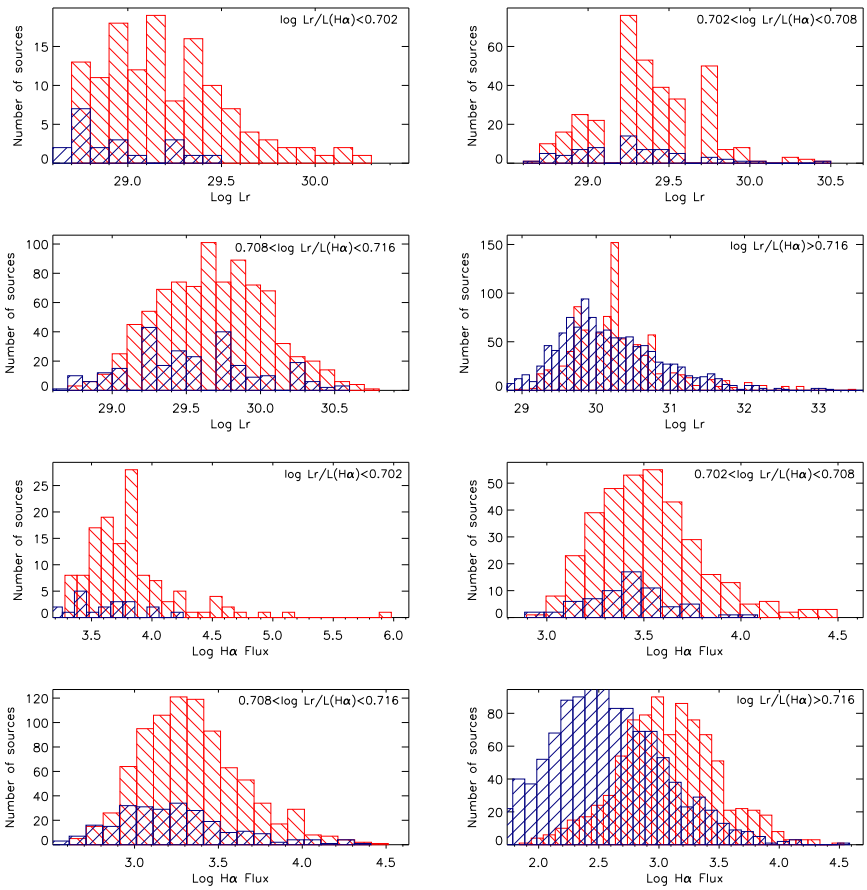

Figure 2: First and second rows: $L_{20\ cm}$ distribution for Seyferts (red) and LINERs (blue) in the four $L_{20\ cm}/L_{H\alpha}$ bins. Third and fourth rows: Hα flux distribution.

4. Results

4.1 Trend with $L_{20\ cm}/L_{H\alpha}$

We study the evolution of the spectroscopic classification of galaxies of the optical-radio sample by placing them in four bins. The bins present increasing $L_{20\ cm}/L_{H\alpha}$ values and contain approximately 2 350 galaxies each. The binning has the purpose of searching for a threshold above which the objects are classified as AGNs (Seyferts or LINERs). The luminosity of the Hα line, $L_{H\alpha}$, is considered to be a good optical star formation rate (SFR) indicator [24]. The ratio between the radio luminosity, $L_{20\ cm}$, and $L_{H\alpha}$ can be used to compare emission from radio components with the emission from young stars. The luminosity of the Hα line has been derived after correcting the corresponding flux for the visual extinction, by using a theoretical Hα/Hβ Balmer ratio of 2.86. Our results are shown in Fig. 1. More diagnostic diagrams and a complete statistical analysis are offered in [25]. The curves separate the three spectroscopic classes of active galaxies. We find that the peak of the distribution shifts from the star-forming (SF) region of the diagrams to the composite (mixed contribution) or AGN part for increasing $\log(L_{20\ cm}/L_{H\alpha})$. In particular, the upper left-hand panels mostly show starbursts with high metallicity, while the bot-

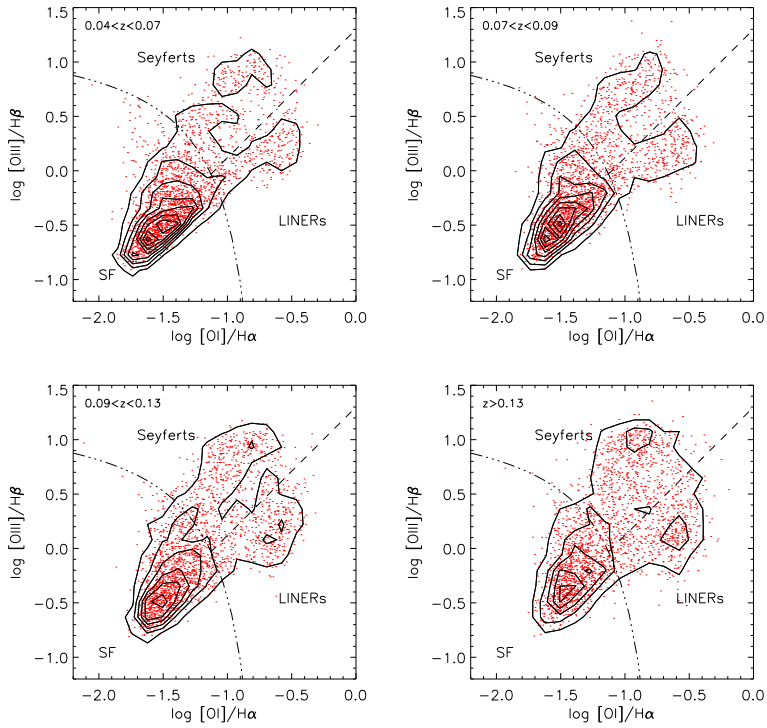

Figure 3: [OI]-based diagnostic diagrams. From top to bottom and from left to right, z increases. The number of radio emitters per bin is constant and equal to $2\,350 \pm 5$. The contours represent the number density of the radio emitters (15 galaxies per density contour).

tom left-hand panels display a mixed population and the bottom right-hand panels show a nearly pure AGN population, together with some metal-rich starbursts. The distribution shows a peak in the LINER region for $\log(L_{20\ cm}/L_{H\alpha}) > 0.716$. In the upper right- and bottom left-hand panels ($0.702 < \log(L_{20\ cm}/L_{H\alpha}) < 0.708$ and $0.708 < \log(L_{20\ cm}/L_{H\alpha}) < 0.716$), the Seyfert region appears increasingly more populated, while the number of Seyfert galaxies remains constant for $\log(L_{20\ cm}/L_{H\alpha}) > 0.716$. In contrast, in the last bin we see an exponential increase in the number of LINERs.

In Fig. 2 (first and second rows) we show the $L_{20\ cm}$ distribution for Seyferts (red) and LINERs (blue) in the four $L_{20\ cm}/L_{H\alpha}$ bins. In the last three bins, the distributions span the same range of values. For $\log(L_{20\ cm}/L_{H\alpha}) > 0.716$, the distributions nearly overlap. In the third and fourth rows of Fig. 2 the Hα flux distribution is shown. The last bin presents a clear dissimilarity in the distribution of Seyferts and LINERs, where the former peaks at higher values. This suggests that the exponential increases in the number of LINERs (Fig. 1, bottom-right panel) is probably due to the lower $L_{H\alpha}$ values that LINERs present compared to Seyferts.

4.2 Trend with redshift

We study the spectroscopic classification as a function of redshift by dividing the sample into four bins containing approximately 2 350 objects each. We find that the distribution of radio emitters in the diagnostic diagrams depends mildly on the redshift (Fig. 3). The number of AGNs

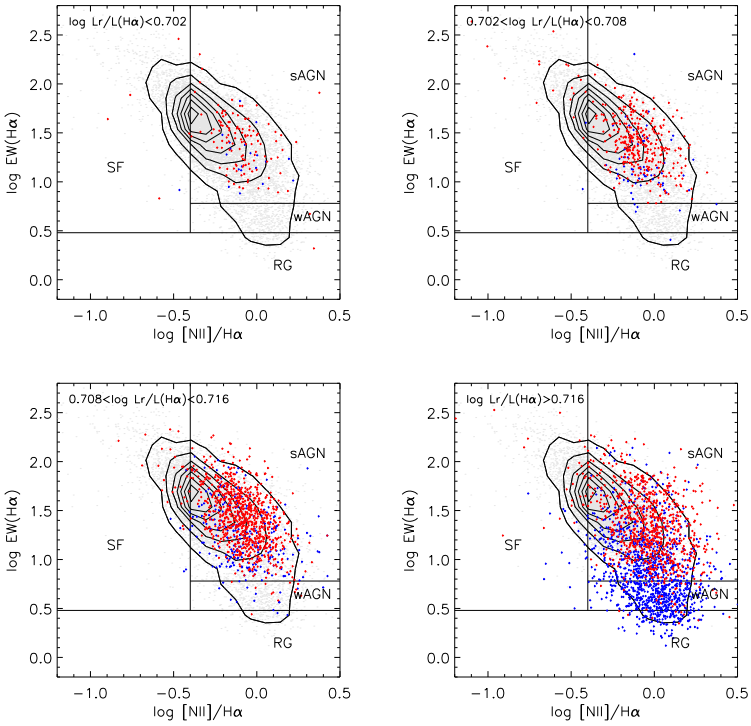

Figure 4: WHAN diagnostic diagrams for the optical-radio sample (light gray) overplotted with Seyferts (red) and LINERs (blue) selected from the [OI]-based diagram. Each plot represents, from the top-left to the bottom-right, a bin with increasing $\log(L_{20\ cm}/L_{H\alpha})$. Contours number density refers to the underlying light gray distribution of each plot and is equal to 70 galaxies per contour.

always increases with z. The bulk of the population remains in the SF region in all z bins. The increase in the number of LINERs and Seyferts show the very same trend. This result points to the possible interpretation that the higher number of AGN we select for increasing redshift is not only due to selection effects (in this case, we would select more powerful sources like Seyferts), but to a combination of the latter with true evolutionary effects.

4.3 Distinguish true from fake AGNs

The question whether LINERs are true AGNs or not still needs to be answered. Emission from some of the galaxies classified as LINERs in the diagnostic diagrams is thought to be triggered by post-asymptotic giant branch stars and white dwarfs, which are abundant in early-type galaxies, classified as 'retired' (RGs) [19]. Weak-line emitting galaxies have been found to have LINER-like emission with $3 <$EW(Hα)$ < 6$ Å in the case of actual LINERs (labeled in the diagram as wAGN, where 'w' stands for 'weak', WHAN diagram [26]) and EW(Hα)$ < 3$ Å for retired galaxies. Galaxies that have both high values of EW(Hα) and [NII]/Hα are classified as strong AGNs (sAGNs).

Figure 4 shows WHAN diagnostic diagrams for the optical-radio sample, overplotted with Seyferts and LINERs selected from the [OI]-based diagram. Each plot represents a different $L_{20\ cm}/L_{H\alpha}$ bin. While the distribution of Seyferts always peaks in the sAGN region, LINERs are mostly present in

the sAGN region in the first three bins, and they appear to be mostly located in the wAGN region in the last $L_{20\ cm}/L_{H\alpha}$ bin. The radio-strong (large $L_{20\ cm}/L_{H\alpha}$) sources deviate from the RG and passive regions.

5. Conclusions

We have combined optical (SDSS DR7) and radio (FIRST) data to conduct a multiwavelength study on the evolution of physical properties of a large sample of radio emitters. We find that AGNs and radio galaxies with AGNs are drawn from a population that has higher metallicity than the overall SDSS sample. The lower abundance objects are predominantly star-forming, and populate the upper left-hand portions of these diagrams.
The connection between optical and radio properties is pointed out by the increasing number of Seyferts and LINERs that we find at high values of $L_{20\ cm}/L_{H\alpha}$ and z. The spectroscopic classification is provided by optical emission-line diagnostic diagrams. The LINER population increases exponentially for the highest values of $L_{20\ cm}/L_{H\alpha}$. LINERs in this luminosity bin present an increase in the radio power of the sources and the drastic drop in their $L_{H\alpha}$. The highest number of Seyferts are found in the third luminosity bin, where the sources present both a high $L_{20\ cm}$ and $L_{H\alpha}$. The progressively and equally higher number of Seyferts and LINERs found at highest z bins possibly indicate that the AGN-detection rate truly correlates with the redshift, besides being due to selection effects. The WHAN diagnostic diagram shows that the galaxies with LINER-like emission are mostly found to present the spectroscopic signatures of actual LINERs (assuming them to be low-luminosity AGNs).

References

[1] D. York et al., *The Sloan Digital Sky Survey: Technical Summary*, *AJ* **120** 1579-1587 [arXiv:astro-ph/0006396]

[2] R. H. Becker et al., *The FIRST Survey: Faint Images of the Radio Sky at Twenty Centimeters*, *APJ* **450** 559

[3] R. Saunders et al., *Spectrophotometry of FRII radiogalaxies in an unbiased, low-redshift sample*, *MNRAS* **238** 777-790

[4] E. L. Zirbel et al., *On the FR I/FR II Dichotomy in Powerful Radio Sources: Analysis of Their Emission-Line and Radio Luminosities*, *APJ* **448** 521

[5] S. A. Baum et al., *Toward Understanding the Fanaroff-Riley Dichotomy in Radio Source Morphology and Power*, *APJ* **451** 88

[6] G. Kauffmann et al., *Radio jets in galaxies with actively accreting black holes: new insights from the SDSS*, *MNRAS* **384** 953-971 [0709.2911]

[7] P. J. McCarthy et al., *High redshift radio galaxies*, *ARAA* **31** 639-688

[8] L. L. Cowie et al., *New Insight on Galaxy Formation and Evolution From Keck Spectroscopy of the Hawaii Deep Fields*, *AJ* **112** 839 [arXiv:astro-ph/9606079]

[9] D. Thomas et al., *The Epochs of Early-Type Galaxy Formation as a Function of Environment*, *APJ* **621** 673-694 [arXiv:astro-ph/0410209]

[10] K. Bundy et al., *The Mass Assembly History of Field Galaxies: Detection of an Evolving Mass Limit for Star-Forming Galaxies*, *APJ* **651** 120-141 [arXiv:astro-ph/0512465]

[11] J. A. Baldwin et al., *Classification parameters for the emission-line spectra of extragalactic objects*, *PASP* **93** 5-19

[12] L. C. Ho et al., *A Reevaluation of the Excitation Mechanism of LINERs*, *APJ* **417** 63

[13] P. F. Hopkins et al., *A Unified, Merger-driven Model of the Origin of Starbursts, Quasars, the Cosmic X-Ray Background, Supermassive Black Holes, and Galaxy Spheroids*, *APJ* **163** 1-49 [arXiv:astro-ph/0506398]

[14] K. N. Abazajian et al., *The Seventh Data Release of the Sloan Digital Sky Survey*, *APJS* **182** 543-558 [0812.0649]

[15] W. OMullane et al., *Batch is back: CasJobs, serving multi-TB data on the Web*, [arXiv:cs/0502072]

[16] L. J. Kewley et al., *The host galaxies and classification of active galactic nuclei*, *MNRAS* **372** 961-976 [arXiv:astro-ph/0605681]

[17] S. Veilleux and D. E. Osterbrock, *Spectral classification of emission-line galaxies*, *APJS* **63** 295-310

[18] F. Lamareille, *The luminosity-metallicity relation in the local Universe from the 2dF Galaxy Redshift Survey*, *MNRAS* **350** 396-406 [arXiv:astro-ph/0401615]

[19] G. Stasińska et al., *Can retired galaxies mimic active galaxies? Clues from the Sloan Digital Sky Survey*, *MNRAS* **391** [L29-L33 0809.1341]

[20] S. A. Baum and T. Heckman, *Extended optical line emitting gas in powerful radio galaxies - What is the radio emission-line connection?*, *APJ* **336** 702-721

[21] R. Morganti et al., *Optical line-emitting gas and radio emission - Evidence for correlation in low-luminosity radio galaxies*, *MNRAS* **254** 546-562

[22] C. N. Tadhunter et al., *The nature of the optical-radio correlations for powerful radio galaxies*, *MNRAS* **298** 1035-1047 [arXiv:astro-ph/9807238]

[23] P. N. Best and T. M. Heckman, *On the fundamental dichotomy in the local radio-AGN population: accretion, evolution and host galaxy properties*, *MNRAS* **421** [1569-1582 1201.2397]

[24] J. Moustakas et al., *Optical Star Formation Rate Indicators*, *APJ* **642** 775-796 [arXiv:astro-ph/0511730]

[25] M. Vitale et al., *Classifying radio emitters from the Sloan Digital Sky Survey. Spectroscopy and diagnostics*, *A&A* **546** A17 [1208.3375]

[26] R. Cid Fernandes et al., *Alternative diagnostic diagrams and the 'forgotten' population of weak line galaxies in the SDSS*, *MNRAS* **403** 1036-1053 [0912.1643]